

Estimating Service Lives of Air-Purifying Respirator Cartridges for Reactive Gas Removal

Gerry O. Wood

Industrial Hygiene and Safety Group, Los Alamos National Laboratory, Los Alamos, New Mexico

A mathematical model has been developed to estimate service lives of air-purifying respirator cartridges that remove gases reactively from flowing air. Most gases, because of their high volatility and low polarizability, are not effectively removed by physical adsorption on activated carbon. Models previously developed for toxic organic vapors cannot estimate service lives of cartridges for toxic gases. Often, an activated carbon is impregnated with a chemical to enhance gas removal by chemical reaction(s). The kinds of reactions, types and amounts of impregnants, and effects of the presence of water vary; therefore, the model requires user inputs of gas capacity and water effect parameters. Ideally, these should be available from manufacturers of the cartridges. If they are not, they can be extracted from measured breakthrough times using this model. The key to this model is the observation that adsorption rates of gases can be adequately quantified by the same correlations that have been reported for organic vapors. The resulting model has been used to correlate and predict breakthrough times for several common toxic gases.

Keywords activated carbon, cartridges, mixtures, organic vapors, respiratory protection

Address correspondence to: Gerry O. Wood, 40 San Juan Street, Los Alamos, NM 87544; e-mail: GerryConsulting@cs.com.

Air-purifying respirators, both negative pressure and powered air-purifying, are sometimes used with cartridges designed to remove specific toxic gases from air to be breathed. Such cartridges usually contain a packed bed of granules of activated carbon impregnated with one or more chemicals. The chemical impregnants are selected to react with or catalyze the decomposition of the gases of concern. Since such reactions are specific for each gas/carbon combination, multiple kinds of impregnated carbons and cartridges are required for the user community.

Reasonable industrial hygiene practice, supported by regulations,⁽¹⁾ requires knowing when gas-removing cartridges are no longer providing a worker with adequate protection. This occurs at the breakthrough time of the gas for a selected breakthrough concentration. The service life is defined as such a breakthrough time with, perhaps, a safety factor

added. Change-out schedules need to be developed and implemented. However, there is little guidance on how to estimate cartridge service lives in actual workplace conditions. Certifications⁽²⁾ verify only that minimum service lives have been achieved in laboratory tests at a set of fixed environmental and testing conditions.

A model⁽³⁾ and computer application⁽⁴⁾ were previously developed for estimating service lives of cartridges designed to remove organic vapors. However, this model is not applicable for the more volatile, usually inorganic gases (such as those in Table I) that do not condense in activated carbon micropores at ordinary use conditions. Therefore, we have undertaken to develop a new model that will make such estimates for cartridges designed for reactive removal of gases.

FUNDAMENTALS

It has long been recognized^(5,6) that a breakthrough curve (concentration of gas exiting a packed carbon bed vs. time of fixed contaminated airflow through it), as illustrated in Figure 1, can be described to a first approximation by what we will generically call the reaction kinetic equation:

$$t_b = \frac{W_e W}{C_o Q} - \frac{W_e \rho_B}{k_v C_o} \ln \left(\frac{C_o - C}{C} \right) \quad (1)$$

It includes (1) carbon bed parameters of bed weight W (g) and packed density ρ_B (g/cm³); (2) parameters of challenge gas concentration C_o (g/cm³), breakthrough concentration C (g/cm³), and airflow rate Q (cm³/min); and (3) gas/carbon interaction parameters of adsorption rate coefficient k_v (min⁻¹) and adsorption capacity W_e (g/g carbon) at C_o . With these units, breakthrough time t_b at breakthrough fraction C/C_o is in minutes.

The first term of Equation 1, $W_e W/C_o Q$, contains the gravimetric equilibrium capacity W_e . While W_e can be calculated⁽³⁾ from chemical and carbon properties (polarizability, adsorption potential, micropore volume, etc.) for organic vapors that have a common adsorption mechanism, no such possibility exists for gases that are each removed by a unique reaction. Only experimental data measured over appropriate ranges of critical parameters (concentration, flow rate, and humidity)

TABLE I. Gas Parameters and Data Sources Used for Examples of Service Life Estimates

Gas	Molecular Weight (g/mol)	Polarizability (cm ³ /mol)	Data Sources (References)
Ammonia	17.03	6.029	11, 17
Chlorine	70.90	11.639	12
Chlorine dioxide	67.46	6.009	22
Cyanogen	52.04	20.155	23
Cyanogen chloride	61.47	12.160	13, 14, 18, 19
Formaldehyde	30.03	6.620	17
Hydrogen cyanide	27.03	6.500	23
Methylamine	31.06	11.000	17
Phosgene	98.92	10.596	24
Sulfur dioxide	64.07	10.090	20, 21

can provide the corresponding gravimetric reaction capacities W_r (g/g) for each gas/carbon combination. Such data are most useful when presented as equations incorporating these critical parameters.

For the calculation of total breakthrough time t_b by Equation 1, the first term, which is called the equilibrium (or stoichiometric) time τ , is reduced by the second term, which contains a first-order adsorption rate coefficient k_v . Both terms must be calculated to get an estimate of a breakthrough time.

BACKGROUND

The adsorption rate coefficient k_v has been well defined for organic vapors on activated carbon. Lodewyckx and Vansant⁽⁷⁾ published an empirical correlation for k_v at 0.1% breakthrough (C/C_o) that included the parameters of affinity coefficient β , linear (superficial, as if the container was empty)

flow velocity v_L (cm/s), and average carbon granule diameter d_p (cm). Wood and Lodewyckx⁽⁸⁾ extended this equation to also incorporate experimental data for gases and for a wider range of concentrations. Inclusion of molar capacity (W_c/M_w , where M_w is the molecular weight) allowed this extended correlation with the result:

$$k_{v0.1\%} = 800\beta^{0.33}v_L^{0.75}d_p^{-1.5}(W_c/M_w)^{0.5} \text{ min}^{-1} \quad (2)$$

Breakthrough curves are often skewed instead of being the symmetrical sigmoid shape predicted by Equation 1 and shown in Figure 1. This means that the apparent k_v is not constant over the breakthrough curve but is a function of the breakthrough fraction C/C_o , as well as other parameters. Wood⁽⁹⁾ has quantified this asymmetry (skew). His equations can be used with Equation 2 to calculate rate coefficients at other breakthrough fractions (up to $C/C_o = 0.5$) as

$$k_{v(C/C_o)} = \left[\frac{1 + b \ln(C_o/C - 1)}{1 + b \ln(999)} \right] k_{v0.1\%} \quad (3)$$

where b is a quadratic root solution of a correlation for the skew parameter $S = k_{v1\%}/k_{v10\%}$:

$$S = \left[\frac{1 + b \ln(99)}{1 + b \ln(9)} \right] \quad (4)$$

$$= 1.41 - 0.0000324 \left[\frac{1 + b \ln(9)}{1 + b \ln(C_o/C - 1)} \right] k_{v(C_o/C)}$$

with a lower limit such that $S \geq 1$.

Adsorption rate coefficients calculated in this way were effective in estimating service lives of cartridges for organic vapors removed by physical adsorption.⁽³⁾ Their application to gases removed by reaction was hypothesized. Observations^(6,7) that organic vapor adsorption rate coefficients are functions of linear flow velocity imply that the rate-controlling step (slowest step in the adsorption process chain) is external mass transfer from the gas (air) phase to the carbon granule surfaces. The dependence of rate coefficients on granular size supports this. Diffusion rate after reaching a granule surface might be size dependent, but it would not be affected by external linear flow velocity. If the rate-controlling step for gases is also external mass transfer, rather than diffusion or reaction, we could expect the above rate coefficient equations to also apply to gas removal by reaction. They would at least provide an upper limit for the rate coefficient.

Lodewyckx et al.⁽¹⁰⁾ have discussed the many ways the Wheeler-Jonas (reaction kinetic) equation can be applied, including for chemisorption. Verhoeven and Lodewyckx⁽¹¹⁾ used it to analyze 25 ppm ammonia breakthrough times vs. carbon weights (Method 2 below) of 70–280 g at breakthrough concentrations of 237–5934 ppm to extract adsorption capacities and rate coefficients. These rate coefficients (3600 min⁻¹ average) were similar to those (2824–3282 min⁻¹) predicted by the original empirical equation reported for physical adsorption of organic vapors.⁽⁷⁾

Lodewyckx and Verhoeven⁽¹²⁾ have similarly applied Equation 1 to chlorine/ASC-TEDA breakthrough time data. (ASC

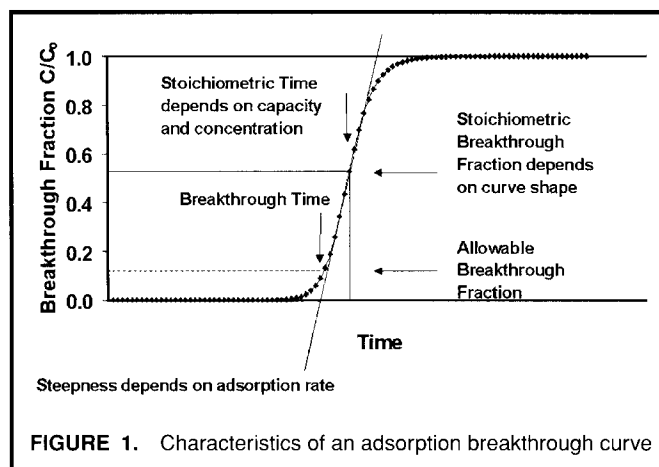


FIGURE 1. Characteristics of an adsorption breakthrough curve

is a carbon impregnated with salts of copper, silver, and chromium; ASC-TEDA is also impregnated with triethylenediamine.) Above 500 ppm the capacity and rate coefficients were apparently independent of concentration and humidity, but increased with airflow velocity. Data at 2000 ppm yielded rate coefficients that were only 10–13% lower than those calculated by Equation 2, the extended empirical rate coefficient equation developed from physical adsorption of organic vapors.⁽⁸⁾

Osmond and Phillips⁽¹³⁾ plotted cyanogen chloride breakthrough times versus ASC-TEDA bed depths to obtain critical bed depths at 1% breakthrough. From these we have derived adsorption rate coefficients increasing from 1445 min⁻¹ at 4.2 cm/sec airflow velocity to 2216 min⁻¹ at 10.6 cm/sec. Corresponding values calculated using Equation 2 for the 8 g/m³ challenge concentration and experimental average capacity of 0.19 g/g range from 2758 min⁻¹ to 5688 min⁻¹.

Staginnus⁽¹⁴⁾ similarly analyzed cyanogen chloride data for a copper- and chromium-impregnated activated peat carbon. The reported experimental rate coefficient of 3370 min⁻¹ compares favorably with 2366 min⁻¹ calculated by Equation 2.

MODEL DESCRIPTION

Drawing on this background as bases for making some assumptions, we have built a mathematical model for estimating service lives of cartridges for reactive gases.

Assumption 1

Since the gases of interest, the types of carbon impregnants, and reactions between them vary widely, we assume there is a reaction capacity, W_r , that can be used in place of adsorption capacity, W_c in Equation 1. The W_r can come only from correlations of experimental data. In the examples below we will show ways of doing this. Gas concentration, water content of the air (relative humidity), and water already on the carbon are often the most critical parameters. However, in some gas/carbon combinations they may have no effect at all.

Assumption 2

For the adsorption rate coefficient k_v at a chosen breakthrough concentration ratio C/C_0 the empirical correlations shown above in Equations 2–4 are assumed. This calculation is very sensitive to the value used for the average granule diameter, d_p , which can depend on size distribution within a size range (e.g., 12–20 mesh) or on shape (see later discussion). Therefore, we assume an “effective granule diameter” (EGD) that can be adjusted from a calculated value of the parameter d_p to better reproduce experimental adsorption rates. It should be considered a property of the carbon used.

Assumption 3

The current model assumes constant (average) challenge concentration, airflow rate, and temperature over the entire period of use. Averages or single point measurements are often all the information that is available from workplace surveys. The extent to which this assumption limits the applicability

of the model if time dependent concentration data is available is yet unknown. Future modifications of the model may allow these parameters to vary with time of cartridge use.

Assumption 4

The affinity (also called by others the “similarity”) coefficient, β , used for calculating the rate coefficient by Equation 2 is defined relative to a reference chemical, taken to be benzene for which $\beta = 1$. For this model it is calculated from a correlation with molar polarizability P_c (cm³/mol),⁽¹⁵⁾

$$\beta = 0.0862P_c^{0.75} \quad (5)$$

Since we are not dealing with liquids, P_c cannot be calculated from refractive index and molar volume; however, it can be calculated from (1) handbook values of polarizability measured in an electric field; or (2) atomic, group, and molecular structure increments.⁽¹⁵⁾ Table I lists the values of P_c we have used for common toxic gases.

Assumption 5

Equation 1 has two terms, each of which can contribute errors and uncertainty to estimating breakthrough times. In the case of the organic vapor model the uncertainty of breakthrough time estimate was found to depend on the ratio of the first two terms of Equation 1.⁽³⁾ In the absence of any such data for gases, this model assumes the standard deviation to be the same function of this ratio.

CAPACITIES FROM EXPERIMENTAL DATA

By Assumption 1, a reactive capacity, W_r , of a specific carbon for a specific gas is required for each gas concentration and humidity. The following paragraphs explain and illustrate several ways in which such capacities can be derived from experimental data. Reaction capacities obtained in one of these ways may vary, depending on (1) the gas concentration, (2) the amount of water present (as relative humidity or adsorbed), and (3) the particular gas/carbon combination. Therefore, measurements (breakthrough curves, breakthrough times, or times vs. weight) need to cover the potential ranges of these parameters in a user's workplace. We suggest a protocol by Wood and Ackley⁽¹⁶⁾ for selecting sets of experimental parameters.

Method 1

Figure 1 shows an idealized complete breakthrough curve and its components. The stoichiometric time can be found from the geometric center of the breakthrough curve by integrating the area above it:

$$\tau = \int_0^\infty (1 - C/C_0) dt \quad (6)$$

This represents the first term of Equation 1, so that reaction capacity W_r for a given set of concentration and humidity conditions can be calculated from τ . Only for a symmetrical breakthrough curve will 50% breakthrough occur exactly at τ , but except for a severely skewed breakthrough curve τ is often close to the 50% breakthrough time. Another advantage

of having at least half a breakthrough curve is that a rate coefficient can be calculated from τ and t_b to determine if the model estimated rate coefficient is reasonable.⁽⁸⁾

Method 2

Another way of obtaining W_r is from the movement of the adsorption wave. This is commonly done by plotting breakthrough time t_b for a fixed breakthrough fraction C/C_0 vs. bed weight W , usually from several experiments varying only bed weight. From Equation 1 the slope of such a linear plot is W_r/QC_0 . The intercept of such a plot yields a rate coefficient but not with much accuracy since the intercept is often close to zero and k_v is obtained from its reciprocal.

Method 3

Equation 1 suggests that plots of t_b vs. $\ln[(C_0 - C)/C]$ should be linear and the capacity W_r should be calculable from the intercept of such a plot. However, this is true only if the breakthrough curve is symmetrical, without skew. Such a plot over a limited C/C_0 range not near 50% may appear to be linear but may not extrapolate to a correct capacity at the stoichiometric center; therefore, this method is not recommended.

Method 4

If only a breakthrough time t_b well below 50% breakthrough is measured, the second term of Equation 1 cannot be known for deriving the first term, τ . However, the model kinetics and rate coefficient estimation (discussed previously) can be assumed in order to calculate τ and W_r from a t_b . With all other parameters put into the model, W_r is varied until the experimental t_b is reproduced. Method 4 has the advantage that any errors in capacity due to estimating the rate coefficient will cancel out when applying the model with the same rate coefficients correlations.

EXAMPLES OF OBTAINING CAPACITIES

Table I lists the sources of data used in the following examples of obtaining capacities by the methods above. In only a few cases have the reported measurements been extensive enough to completely define the effects of gas concentration and/or water. As stated previously, the parameters derived from one gas/carbon combination are not likely to apply to another. Therefore, the following should be considered as examples only.

Ammonia Examples

Verhoeven and Lodewyckx⁽¹¹⁾ published test parameters and breakthrough times for 237–5934 ppm ammonia in air passed through packed beds of Chemviron ASC-TEDA carbon. The breakthrough concentration was selected as 25 ppm and the packed carbon bed density was 0.56 g/cm³. Fourteen experiments used dry cartridges and either dry or 70% RH air. We used Method 4 above with our proposed model to calculate ammonia capacities ranging from 0.0076 to 0.0174 g/g. Figure 2 shows that within the precision of the results there

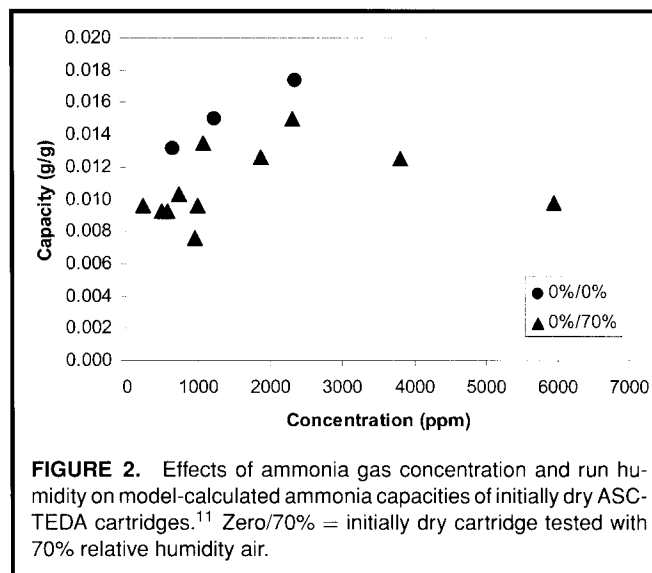


FIGURE 2. Effects of ammonia gas concentration and run humidity on model-calculated ammonia capacities of initially dry ASC-TEDA cartridges.¹¹ Zero/70% = initially dry cartridge tested with 70% relative humidity air.

are no apparent trends due to ammonia concentration or air humidity. The value of capacity that gave the best agreement of estimated breakthrough times with experimental ones for the dry cartridges (Figure 3) was 0.0097 g/g. However, for the prewetted cartridges run at each preconditioning humidity (30–90% RH) capacities calculated from breakthrough times were significantly higher (Figure 4). The polynomial correlation that summarizes all these capacity results is given in Figure 4. Figure 3 shows the agreements of model estimates and experiments for both sets of data.

An MSA database contains cartridge parameters and 25 ppm ammonia breakthrough times for 100–300 ppm at 25–75% RH for two sizes of GME cartridges, tested as received.⁽¹⁷⁾ (GME is a designation of a series of cartridges manufactured by MSA, Inc., Pittsburgh, Pa., containing a proprietary carbon and approved for removal of a variety of gases and organic vapors.) Method 4 was used with this data to extract reaction capacities. In this case, an effect of ammonia concentration on reaction capacity was clear (Figure 5). The correlation in

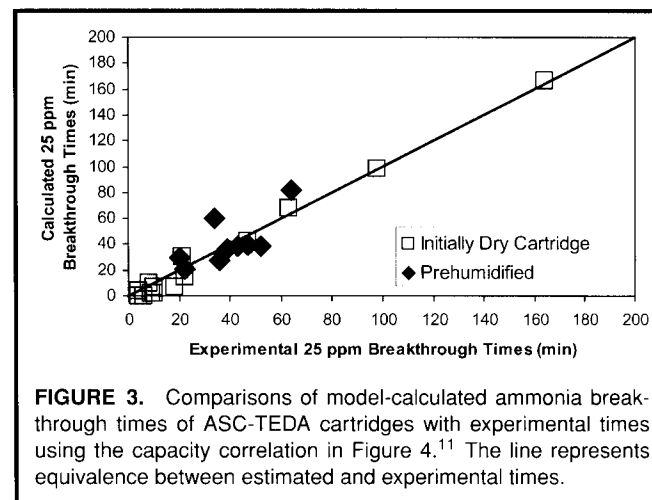


FIGURE 3. Comparisons of model-calculated ammonia breakthrough times of ASC-TEDA cartridges with experimental times using the capacity correlation in Figure 4.¹¹ The line represents equivalence between estimated and experimental times.

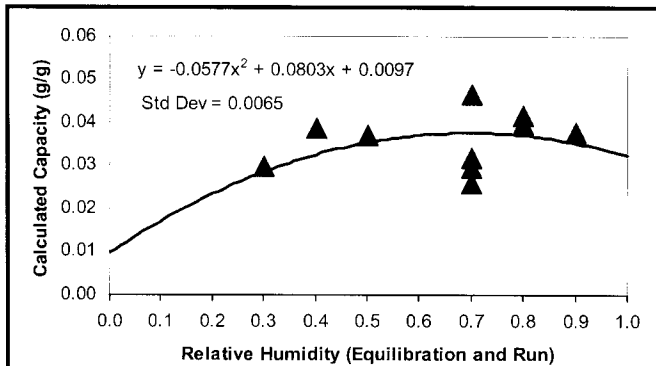


FIGURE 4. Capacities calculated by the model from ammonia breakthrough times for ASC-TEDA cartridges vs. equilibration (and Run) relative humidities.¹¹ The line represents a polynomial equation least-squares fit with intercept forced to 0.0097, the value found to be optimum in Figure 3 for the initially dry cartridges.

Figure 5 reproduces experimental results quite well (Figure 6) for both cartridges, independent of air humidity up to 75% RH.

Chlorine Examples

Lodewyckx and Verhoeven⁽¹²⁾ studied chlorine removal by ASC-TEDA, ASC, and BPL (an activated, unimpregnated carbon). By Method 2 they obtained an average capacity of 0.13 g/g for the ASC-TEDA, apparently independent of concentration and relative humidity (preconditioning and/or use) up to 70%. Using this capacity with breakthrough times at various concentrations (220–3408 ppm) they calculated rate coefficients from Equation 1. These rate coefficients seemed to average 3000 min⁻¹ for concentrations above 1000 ppm, but increase rapidly below 1000 ppm.

We have done our own analysis of this data using Method 4. First, we noticed that the micropore volumes and capacities on a volumetric (e.g., W_r times ρ_B in g/cm³) basis were essentially the same for all three carbons. This implies that the impregnants have nothing to do with chlorine removal, but only change the weight and, therefore, the density of the carbon. Next,

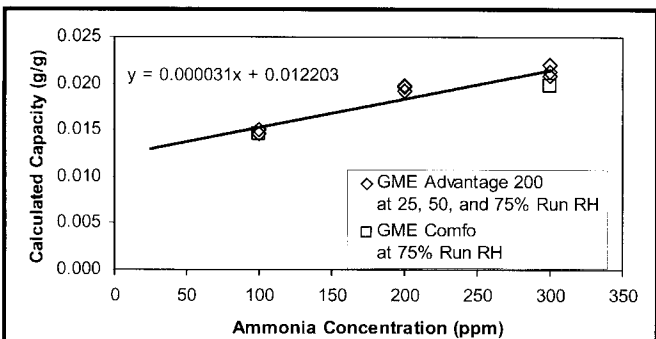


FIGURE 5. Capacities calculated by the model from ammonia breakthrough times for two sizes of GME cartridges vs. concentrations for cartridges tested as received with 25–75% RH air.¹⁷ The line and its equation are the best fit (linear least squares) through the data.

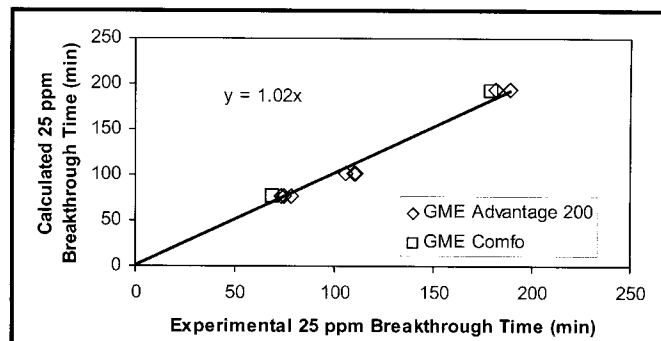


FIGURE 6. Comparisons of model-calculated ammonia breakthrough times of GME cartridges with experimental ones using the capacity correlation in Figure 5.¹⁷ The best fit (linear least squares) line through the origin shows agreement within 2%.

we discovered that chlorine reaction capacity increased with breakthrough time for all the carbons at all humidity conditions (Figure 7). We attribute this to a fast reaction with capacity 0.075 g/cm³ (intercept of Figure 7) and a slower reaction producing the slope. The linear correlation resulted in the good agreement of estimated breakthrough times with experimental ones shown in Figure 8.

Cyanogen Chloride Examples

Osmond and Phillip⁽¹³⁾ published breakthrough times analyzed by Method 2 to get wave movement rates (a in min/cm) and critical bed depths (in cm for 1% breakthrough) for cyanogen chloride on an ASC-TEDA carbon at 80% RH. The values of a yield an average reaction capacity of 0.19 g/g, apparently independent of airflow velocity (4.2–10.6 cm/sec), bed depth (1.5–3 cm), and concentration (4–8 g/m³). Rate coefficients we have calculated from their critical bed depths average 45% lower than those predicted by our model. This discrepancy could indicate that (1) the cyanogen chloride removal rate is slower than the external mass transfer rate, (2) the

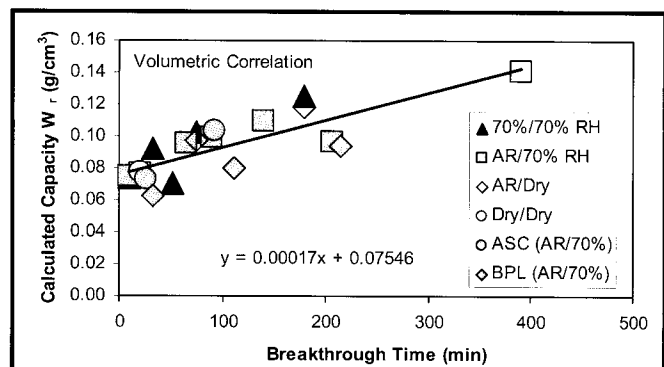


FIGURE 7. The effect of chlorine gas breakthrough times on model-calculated volumetric capacities for various carbons and humidity conditions.¹² Unless noted otherwise, the results are for ASC-TEDA carbon. The line and its equation represent the best linear least squares fit of the data.

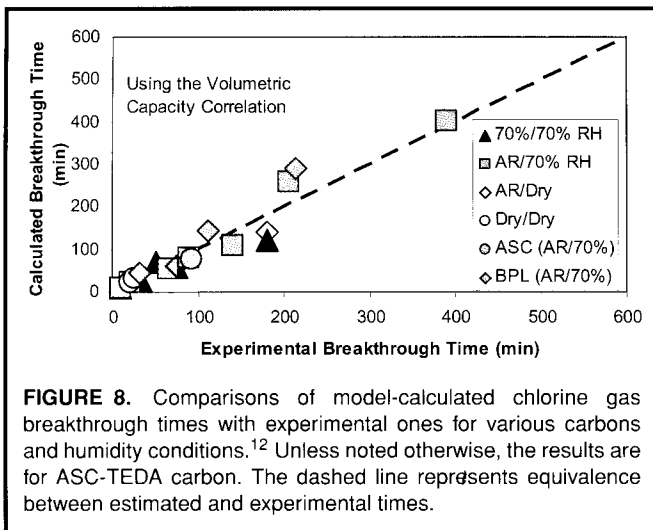


FIGURE 8. Comparisons of model-calculated chlorine gas breakthrough times with experimental ones for various carbons and humidity conditions.¹² Unless noted otherwise, the results are for ASC-TEDA carbon. The dashed line represents equivalence between estimated and experimental times.

capacity is lower and not constant, or (3) the EGD is larger than calculated from the reported 12–30 mesh range.

We have tried two alternative analyses of these data. First, we used Method 4 to calculate capacities from breakthrough times and the model rate coefficients. A correlation of such capacities is shown in Figure 9. Second, we used a fixed 0.19 g/g capacity with an EGD of 0.17 cm, instead of 0.10 cm (calculated from the mesh size range) and calculated breakthrough times. Both approaches produced breakthrough time results in good agreement with each other and with the correlation of Osmond and Phillips (Figure 10 includes data from Table VI of Reference 13). The model is useful for estimations using any of these approaches.

The Staginnus breakthrough times for cyanogen chloride on 6.5-cm diameter beds of a copper- and chromium-impregnated activated peat carbon (dry conditions) were obtained from his published graphs.¹⁴ A Method 4 analysis yielded a capacity of 0.059 g/g at 2 g/m³ concentration, independent of flow rate (10–46 L/min) and bed depth (1–3.5 cm). This is in agreement with (1) the intercept of Figure 9, (2) an average value of 0.058 g/g

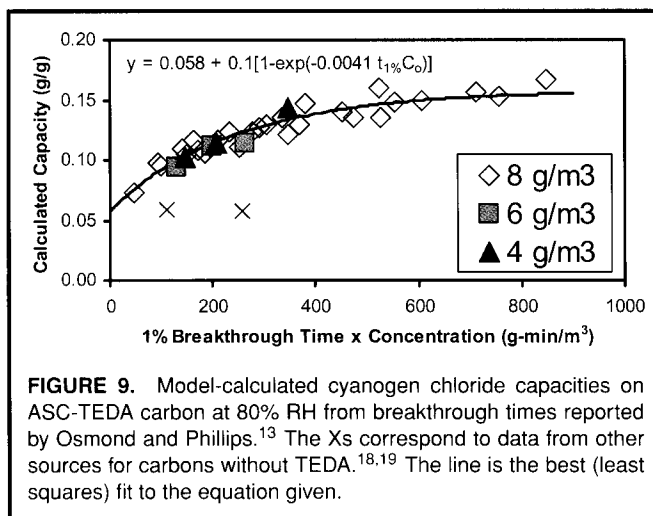


FIGURE 9. Model-calculated cyanogen chloride capacities on ASC-TEDA carbon at 80% RH from breakthrough times reported by Osmond and Phillips.¹³ The Xs correspond to data from other sources for carbons without TEDA.^{18,19} The line is the best (least squares) fit to the equation given.

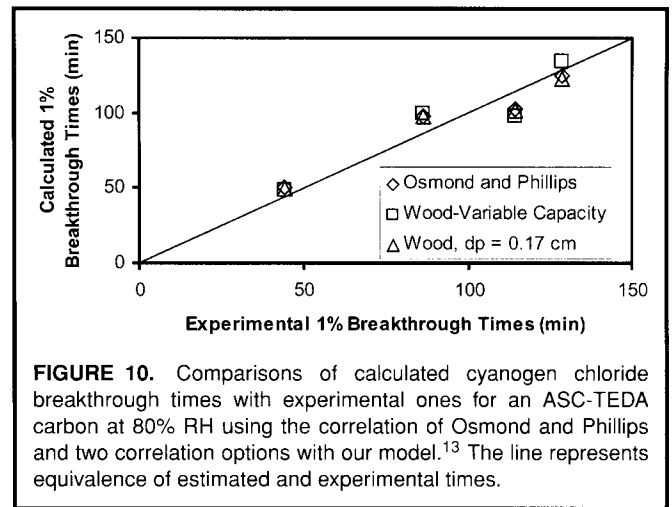


FIGURE 10. Comparisons of calculated cyanogen chloride breakthrough times with experimental ones for an ASC-TEDA carbon at 80% RH using the correlation of Osmond and Phillips and two correlation options with our model.¹³ The line represents equivalence of estimated and experimental times.

at 4 g/m³ we derived by Method 4 from breakthrough times of Deitz with an ASC carbon equilibrated and run at 80% RH,⁽¹⁸⁾ and (3) an average value of 0.058 g/g at 2.4 g/m³ from the work of Aharoni and Barnir⁽¹⁹⁾ for two dry copper/chromium-impregnated carbons run at 75% RH. This suggests that the intercept of Figure 9 is due to a fast reaction and the capacity increase is due to a slower reaction with the TEDA present. Figure 11 shows the model agreement with Staginnus' breakthrough times using 0.059 g/g.

Sulfur Dioxide Examples

Perrard et al.⁽²⁰⁾ studied the breakthrough of sulfur dioxide on a commercial extruded Norit Rox 0.8 carbon, a crushed and sieved sample of it, and an activated carbon fibrous felt. They applied what we have called Methods 1, 2, and 3 to get capacities and rate coefficients. Carbon capacities ranged 0.003–0.006 g/g at 9.1 ppm for the activated carbons and 0.019–0.024 g/g at 31.2 ppm for the activated felt. Assuming a temperature of 20°C, we used these reported capacities

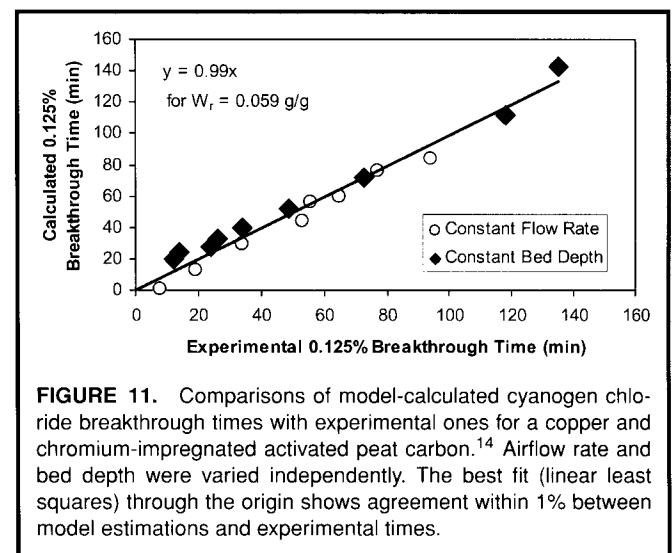


FIGURE 11. Comparisons of model-calculated cyanogen chloride breakthrough times with experimental ones for a copper and chromium-impregnated activated peat carbon.¹⁴ Airflow rate and bed depth were varied independently. The best fit (linear least squares) through the origin shows agreement within 1% between model estimations and experimental times.

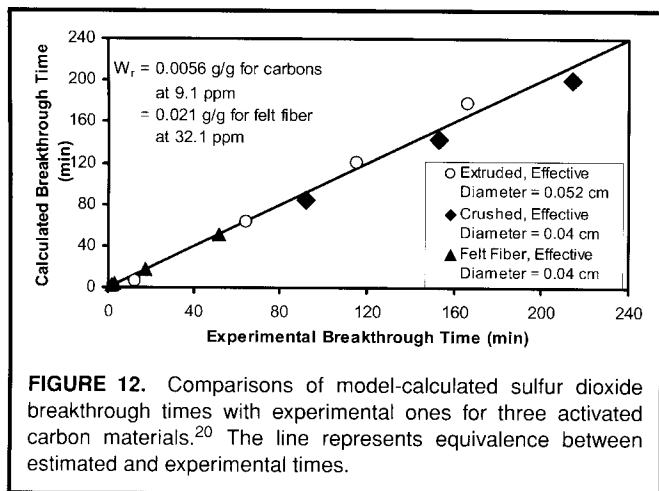


FIGURE 12. Comparisons of model-calculated sulfur dioxide breakthrough times with experimental ones for three activated carbon materials.²⁰ The line represents equivalence between estimated and experimental times.

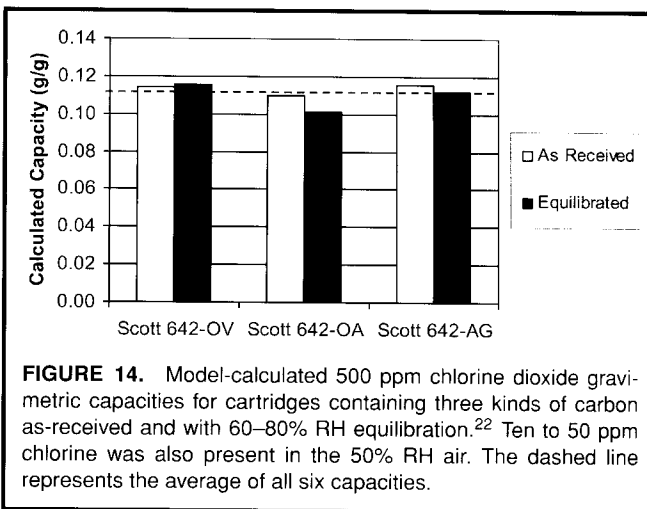


FIGURE 14. Model-calculated 500 ppm chlorine dioxide gravimetric capacities for cartridges containing three kinds of carbon as-received and with 60–80% RH equilibration.²² Ten to 50 ppm chlorine was also present in the 50% RH air. The dashed line represents the average of all six capacities.

and rate coefficients to back-calculate the experimental 1.5% breakthrough times for various bed weights. Figure 12 shows the agreement of model estimates for the extruded carbon, crushed sample, and activated felt fiber using capacities of 0.0056 g/g, 0.0056 g/g, and 0.021 g/g and EGDs of 0.052, 0.04, and 0.04 cm, respectively.

In a related paper, Martin et al.⁽²¹⁾ showed that the adsorption of SO₂ on the extruded Norit Rox 0.8 carbon is partially reversible and partially irreversible, both capacities increasing with concentration. Since it is the total that is important for a single-use respirator cartridge, we have used the capacity totals taken from our analysis in the previous paragraph and from Reference 21 for as-received carbons to get the capacity vs. concentration correlation shown in Figure 13. Martin et al.⁽²¹⁾ found that drying the as-received carbon to remove water actually decreased the capacity of the carbon for sulfur dioxide. Effects of added amounts of water or high humidities on SO₂ capacities have not been quantified or explained.

Chlorine Dioxide Example

Simon et al.⁽²²⁾ evaluated a variety of respirator cartridges for removal of (500 ± 50 ppm) chlorine dioxide in 50% RH

air also containing 10–50 ppm chlorine. Cartridges were tested for 0.46 ppm ClO₂ breakthrough times both as-received and initially equilibrated (60–80% RH). The three Scott 642 cartridges (OV = organic vapor, OA = organic vapor/acid gas, and AG = acid gas) contained the same volume of carbon, but increasing (OV to OA to AG) weights of carbon presumably due to an increasing presence of impregnants. The manufacturer (personal communication, M. Riggs, Scott Health and Safety, January 2004) has provided us with carbon bed geometries and ranges of weights from which we obtained averages to use in the model with Method 4. The resulting gravimetric capacities (averaging 0.112 g/g carbon for the three cartridges) show (Figure 14) no consistent differences due to humidity equilibration. Since there are also no large differences among the three types of cartridges, this might seem to indicate no effectiveness of the impregnants. However, on a volumetric basis (g/cm³ carbon) the capacity clearly (Figure 15) increases with the amount of acid-gas impregnants. Since cartridges usually have a fixed bed volume, such volume-based differences are important and demonstrate the effectiveness of impregnants.

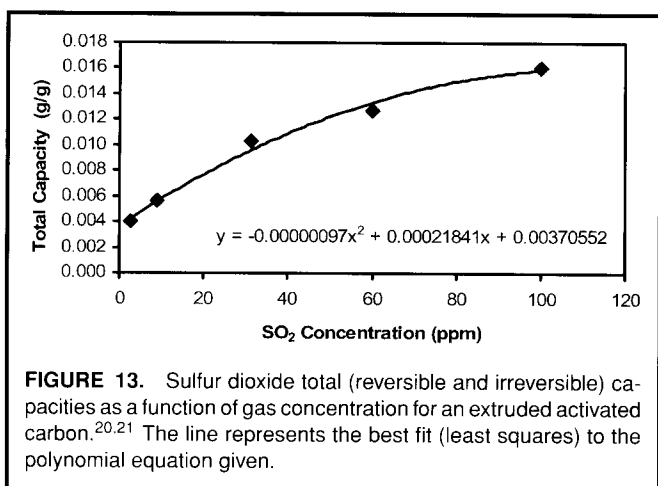


FIGURE 13. Sulfur dioxide total (reversible and irreversible) capacities as a function of gas concentration for an extruded activated carbon.^{20,21} The line represents the best fit (least squares) to the polynomial equation given.

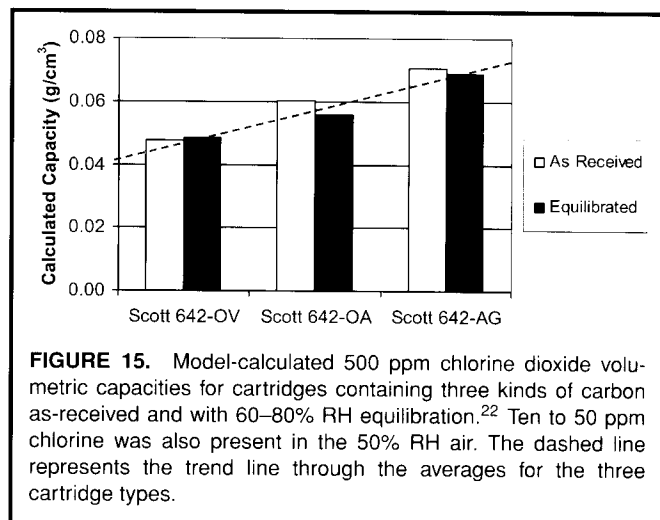


FIGURE 15. Model-calculated 500 ppm chlorine dioxide volumetric capacities for cartridges containing three kinds of carbon as-received and with 60–80% RH equilibration.²² Ten to 50 ppm chlorine was also present in the 50% RH air. The dashed line represents the trend line through the averages for the three cartridge types.

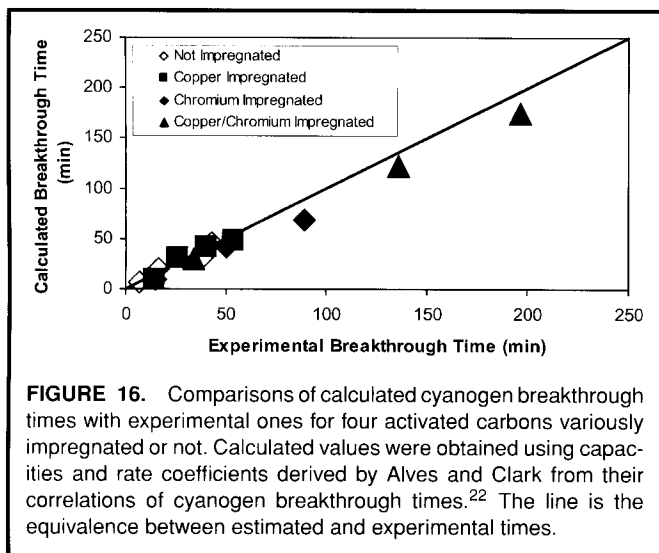


FIGURE 16. Comparisons of calculated cyanogen breakthrough times with experimental ones for four activated carbons variously impregnated or not. Calculated values were obtained using capacities and rate coefficients derived by Alves and Clark from their correlations of cyanogen breakthrough times.²² The line is the equivalence between estimated and experimental times.

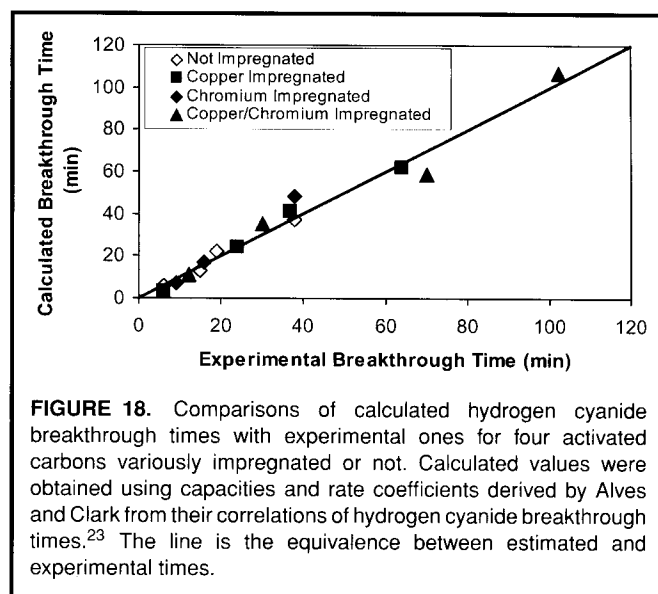


FIGURE 18. Comparisons of calculated hydrogen cyanide breakthrough times with experimental ones for four activated carbons variously impregnated or not. Calculated values were obtained using capacities and rate coefficients derived by Alves and Clark from their correlations of hydrogen cyanide breakthrough times.²³ The line is the equivalence between estimated and experimental times.

Hydrogen Cyanide and Cyanogen Examples

Alves and Clark⁽²³⁾ studied the effects of copper and chromium salt impregnants on the removals of hydrogen cyanide and cyanogen by activated carbon. Cyanogen and hydrogen cyanide concentrations were 1 and 2 g/m³ (463 and 1780 ppm), respectively; breakthrough concentration was defined as 0.001 g/m³. They analyzed breakthrough time data by Method 2 to get capacities and rate coefficients for each of four carbons. We have taken breakthrough times from their plots vs. bed weights and analyzed them by our model with Method 4. Bed densities (0.43–0.57 g/cm³) were back-calculated from reported capacities and carbon weights. We assumed an EGD of 0.10 cm (for reported 16–22 mesh) and temperature of 20 C.

Figure 16 shows breakthrough times for cyanogen calculated from Alves and Clark's reported capacities and rate coefficients vs. experimental times taken from their graphs. Figure 17 shows the same for our model with capacities 0.0163 g/g (unimpregnated carbon), 0.0221 g/g (copper impregnated),

0.0315 g/g (chromium impregnated), and 0.0610 g/g (copper and chromium impregnated). Likewise, Figures 18 and 19 compare Alves and Clark's hydrogen cyanide correlations with those of our model for capacities 0.013 g/g, 0.029 g/g, 0.013 g/g, and 0.056 g/g, respectively. While some of their correlation estimates were better (higher) for short breakthrough times, the ones from our proposed model were often closer to the experimental times at longer times more useful in respiratory protection applications.

Examples Demonstrating Limitations

The MSA database also includes 10 ppm breakthrough time data for 100 ppm methylamine and several cartridges.⁽¹⁷⁾ As expected for this water-soluble gas, breakthrough times increased with air humidity. Applying the model to GMA Advantage 200 cartridges, we calculated capacities of 0.014 g/g, 0.021 g/g, and 0.036 g/g at relative humidities of <10%, 50%, and 90%, respectively. The GME carbon capacity increased

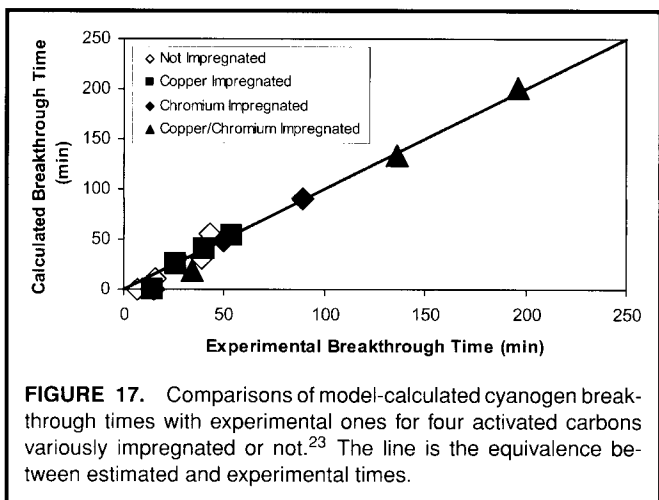


FIGURE 17. Comparisons of model-calculated cyanogen breakthrough times with experimental ones for four activated carbons variously impregnated or not.²³ The line is the equivalence between estimated and experimental times.

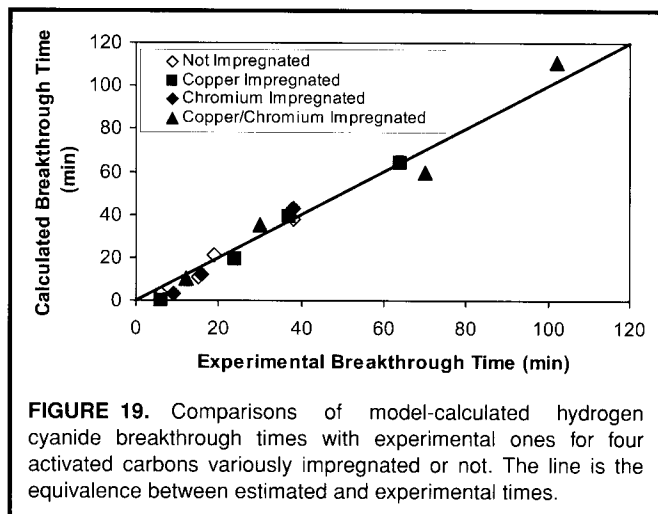


FIGURE 19. Comparisons of model-calculated hydrogen cyanide breakthrough times with experimental ones for four activated carbons variously impregnated or not. The line is the equivalence between estimated and experimental times.

from 0.038 g/g at <10% RH to 0.070 g/g at 50% RH. Until there are data to determine effects of methylamine concentration, these capacities must be used with care.

The same database lists two 0.75 ppm breakthrough times for 10 ppm formaldehyde on two kinds of GME cartridges at 50% RH.⁽¹⁷⁾ Applying our model these times correspond to 0.009 ± 0.003 g/g capacity. However, capacities at other concentrations and humidity conditions are not known or derivable from this limited data.

One case in which the model and Method 4 did not work was with phosgene on an ASC-TEDA carbon.⁽²⁴⁾ In this study temperature rises well above ambient were observed for the high concentrations (5200–21300 ppm) used. The current model cannot predict these temperatures or take them into account.

DISCUSSION AND CONCLUSIONS

The assumptions made, in particular assuming published external mass transfer rate coefficient correlations, have resulted in a model useful for correlating breakthrough data and estimating service lives (breakthrough times at chosen breakthrough concentrations) of gas-removing, air-purifying respirator cartridges, canisters, and other packed carbon beds.

However, the model first requires reaction capacities and correlations specific for each gas and cartridge carbon combination. Such data and correlations can be obtained from breakthrough time data, as we have demonstrated. We have seldom found breakthrough times extensive enough to determine both gas concentration and relative humidity effects. We recommend that such data be developed or released, if they are unpublished.

Our examples show how this model can be used to extract such needed reaction capacities from experimental breakthrough curves or breakthrough times. Another application of this model is in the design of cartridges and canisters containing them by varying the bed parameters (depth, diameter, granule size) and observing the effects on breakthrough times.

It must be reiterated that there are potentially large errors in breakthrough time (service life) estimates if capacity data are used for concentrations well outside the range from which such capacities were derived. The same caution applies to extrapolating outside of experimental relative humidity ranges.

A computer program can be written to implement the gas removal model. It might be similar to the one we have written for the organic vapor model.⁽⁴⁾ However, its usefulness will depend on having the needed input parameters for actual commercial cartridges and the impregnated carbons they contain.

ACKNOWLEDGMENTS

This work was performed at the Los Alamos National Laboratory under the auspices of the U.S. Department of Energy and was funded by the National Personal Protective Technology Laboratory of the National Institute for Occu-

pational Safety and Health, Centers for Disease Control and Prevention, U.S. Department of Health and Human Services, Pittsburgh, Pennsylvania.

REFERENCES

1. "Respiratory Protection, Final Rule." *Federal Register* 63:1152–1300 (8 January 1998).
2. "Revision of Tests and Requirements for Certification of Permissibility of Respiratory Protective Devices Used in Mines and Mining." *Federal Register* 52:32402–32443 (27 August 1987).
3. Wood, G.O.: Estimating service lives of organic vapor cartridges II: A single vapor at all humidities. *J. Occup. Environ. Hyg.* 1:472–492 (2004).
4. "Breakthrough: Single Vapor Version 3.0.2, September 2004." [Online] Available at http://www.osha.gov/SLTC/etools/respiratory/advisor_genius_wood/breakthrough.html (Accessed December 2004).
5. Wood, G.O.: *Reviews of Models for Adsorption of Single Vapors, Mixtures of Vapors, and Vapors at High Humidities on Activated Carbon for Applications Including Predicting Service Lives of Organic Vapor Respirator Cartridges*. Report LA-UR-00-1531, Los Alamos, NM: Los Alamos National Laboratory, 2000.
6. Wood, G.O., and E.S. Moyer: A review of the Wheeler equation and comparison of its applications to organic vapor respirator cartridge breakthrough data. *Am. Ind. Hyg. Assoc. J.* 50:400–407 (1989).
7. Lodewyckx, P., and E.F. Vansant: Estimating the overall mass transfer coefficient k_v of the Wheeler-Jonas equation: A new and simple model. *Am. Ind. Hyg. Assoc. J.* 61:501–505 (2000).
8. Wood, G.O., and P. Lodewyckx: An extended equation for rate coefficients for adsorption of organic vapors and gases on activated carbons in air-purifying respirator cartridges. *Am. Ind. Hyg. Assoc. J.* 64:646–650 (2003).
9. Wood, G.O.: Quantification and application of skew of breakthrough curves for gases and vapors eluting from activated carbon beds. *Carbon* 40:1883–1890 (2002).
10. Lodewyckx, P., G.O. Wood, and S.K. Ryu: The Wheeler-Jonas equation: A versatile tool for the prediction of carbon bed breakthrough times. In *Carbon '03, An International Carbon Conference, Oviedo, Spain, July 6–10, 2003*. Saragossa, Spain: Spanish Carbon Group, 2003.
11. Verhoeven, L., and P. Lodewyckx: Using the Wheeler-Jonas equation to describe adsorption of inorganic molecules: Ammonia. In *Proceedings of CARBON '01, Biennial Conference on Carbon*. Lexington, Kentucky, July 14–19, 2001. Philadelphia: American Carbon Society, 2002.
12. Lodewyckx, P., and L. Verhoeven: Using the modified Wheeler-Jonas equation to describe the adsorption of inorganic molecules: Chlorine. *Carbon* 41:1215–1219 (2003).
13. Osmond, N.M., and P.L. Phillips: Pressure drop and service life predictions for respirator canisters. *Am. Ind. Hyg. Assoc. J.* 62:288–294 (2001).
14. Staginnus, B.: Adsorption of cyanogen chloride and chloropicrin on activated carbon. In *Extended Abstracts of the 15th Biennial Conference on Carbon*. Philadelphia: American Carbon Society, 1981. pp. 228–229.
15. Wood, G.O.: Affinity coefficients of the Polanyi/Dubinin adsorption isotherm equations. A review with compilations and correlations. *Carbon* 39:343–356 (2001).
16. Wood, G.O., and M.W. Ackley: A testing protocol for organic vapor respirator canisters and cartridges. *Am. Ind. Hyg. Assoc. J.* 50:651–654 (1989).
17. Mine Safety Appliances Company (MSA): Respirator test data. [Online] Available at www.msanet.com (Accessed October 27, 1999).
18. Deitz, V.: *Chemistry and Physics of Surfaces—Collective and Individual Protection, Quarterly Report—January–March 1986*. Report CRDEC-CR-87075. Washington, D.C.: Naval Research Laboratory, 1987.

19. **Aharoni, C., and Z. Barnir:** Efficiency of adsorbents for the removal of cyanogen chloride. *Am. Ind. Hyg. Assoc. J.* 39:334–339 (1978).
20. **Perrard, A., J.-P. Joly, and C. Martin:** The Wheeler-Jonas model for interpreting breakthrough curves of SO₂ traces in air through carbon beds. *Proceedings of Carbon '03, An International Carbon Conference, Oviedo, Spain, July 6–10, 2003.* Saragossa, Spain: Spanish Carbon Group, 2003.
21. **Martin, C., A. Perrard, J.P. Joly, F. Gaillard, V. Delecroix:** Dynamic adsorption on activated carbons of SO₂ traces in air I. Adsorption capacities. *Carbon* 40:2235–2246 (2002).
22. **Simon, C.G., R.P. Fisher, and J.D. Davison:** Evaluation of respirator cartridges for effectiveness of chlorine dioxide removal. *Am. Ind. Hyg. Assoc. J.* 48:1–8 (1987).
23. **Alves, B.R., and A.J. Clark:** An examination of the products formed on reaction of hydrogen cyanide and cyanogen with copper, chromium (6+) and copper-chromium (6+) impregnated activated carbons. *Carbon* 24:287–294 (1986).
24. **Verhoeven, L., D. Van Rompaey, and P. Lodewyckx:** The temperature effects of the adsorption of phosgene on military filters. *Proceedings of CARBON '01, Biennial Conference on Carbon, Lexington, Kentucky, July 14–19, 2001.* Philadelphia: American Carbon Society, 2002.